J Solid State Electrochem (2000) 4: 205–209 © Springer-Verlag 2000

ORIGINAL PAPER

Shinichi Waki · Kaoru Dokko · Takashi Itoh
Matsuhiko Nishizawa · Takayuki Abe · Isamu Uchida

High-Speed voltammetry of Mn-doped $LiCoO_2$ using a microelectrode technique

Received: 7 June 1999 / Accepted: 25 June 1999

Abstract The microelectrode technique was applied to investigate the electrochemical properties of $LiCo_{1-x}Mn_xO_2$ ($x = 0$, 0.01, 0.05, 0.2, or 0.5) synthesized using the citrate process. From the X-ray diffraction measurements, an expansion of the *c*-axis and a decrease in the crystal size of the materials were observed on substitution of Mn into $LiCoO_2$. In the electrochemical measurements, the high-speed cyclic voltammogram for the Mn-substituted materials gave one set of peaks at 3.9 V vs. Li/Li^+. The apparent chemical diffusion constant (D_{app}) of $LiCo_{0.8}Mn_{0.2}O_2$ obtained from the potential step experiment was 6.4×10^{-8} cm^2/s, which is larger than that of $LiCoO_2$. The increase in D_{app} is attributable to the expansion of the *c*-axis and/or the decrease in the crystal size. In addition, the increase in Mn substitution up to 20% lead to an improvement in the kinetic reversibility and the cycle stability of $LiCoO_2$.

Key words High speed voltammetry · Lithium cobalt oxide · Manganese substitution · Kinetic reversibility · Cycle stability

Introduction

$LiCoO_2$ has been presently commercialized as the cathode material of the lithium ion secondary battery [1, 2]. While $LiCoO_2$ has a high potential of ca. 4 V vs. Li/Li^+ in its extraction form and has excellent reversibility for Li insertion/extraction, several attempts to improve its electrochemical characteristics by substituting part of the Co with other metallic elements (M = Mg, Cr, Mn, or Ni) are still being studied [3–8]. For example, Tukamoto and West [3] have reported that the electron conductivity was improved by substituting Mg into $LiCoO_2$. With Mn-substituted $LiCoO_2$, Stoyanova et al. [4] and Iltchev et al. [5] have claimed improvement in the cycle life and discharge capacity. Jones et al. [6] have reported that $LiCoO_2$ with a small amount of chromium showed poor cycling behavior. Ohzuku et al. [7, 8] have reported that the open-circuit voltages varied as a function of *x* in $LiNi_{1-x}Co_xO_2$. In these investigations, however, since the composite electrodes (consisting of the powdery active material and some additives) have been used for measuring the electrochemical properties of the active materials, it is difficult to reveal the electrochemical characteristics of only the materials.

On the other hand, we have recently developed an electrochemical measurement method for a single particle of battery active materials using a microelectrode technique. We have demonstrated its ability to evaluate the electrochemistry characteristics of active materials alone, without any influence of a binder and electric conduction additives such as carbon, by this technique [9–15]. In addition, the small amplitude of the observed current in the microelectrode system improves the distortion of voltammograms due to *iR* drop, thus allowing the conventional electrochemical analyses to be used, which allows us to discuss the mechanism of Li^+ insertion/extraction.

In this paper, Mn-substituted $LiCoO_2$, which seems to improve the electrochemical properties of $LiCoO_2$ [4, 5], was prepared and its unique electrochemical characteristics were measured by cyclic voltammetry and potential step experiments with a microelectrode. In this study, we have revealed the electrochemical properties of the Mn-substituted materials alone and have found that a remarkable improvement in the kinetic reversibility and the cycle stability was observed for $LiCo_{0.8}Mn_{0.2}O_2$.

S. Waki · K. Dokko · T. Itoh · M. Nishizawa · T. Abe
I. Uchida (✉)
Department of Applied Chemistry,
Graduate School of Engineering,
Tohoku University, Aramaki-Aoba,
Aoba-ku, Sendai 980-8579, Japan
e-mail: uchida@est.che.tohoku.ac.jp
Tel.: +81-22-2177220;
Fax: +81-22-2148646

Experimental

Samples used in this work were synthesized using the so-called "citrate process" (see, for example, [16]). Briefly, stoichiometric amounts of $LiNO_3$, $Co(NO_3)_2$, and $Mn(NO_3) \cdot 6\ H_2O$ were dissolved in distilled water containing citric acid (twice the $LiNO_3$ amount). The resulting solution was then evaporated in a rotary evaporator at 60 °C. The resultant viscous solution was further evaporated at 80 °C for at least 24 h. The pink powdery precursor of the citrate complex was obtained. The final products, $LiCo_{1-x}Mn_xO_2$ ($x = 0$, 0.01, 0.05, 0.2, or 0.5), were obtained from the calcination of the resultant precursor at 700 °C for 12 h in oxygen. Atomic absorption analysis (Perkin Elmer, model 3300) showed that the atomic ratios of Mn:Co in the final products were almost the same as those in the synthetic solution, within experimental error. Structural information of the samples was obtained by powder X-ray diffraction (XRD) analysis using a Shimadu XD-D1 with Cu-Kα radiation with divergent and receiving slits of 0.3 mm. The lattice constant of the samples was calculated by the Nelson-Riley least-squares method on the LCR2 program. The BET surface area was calculated from a N_2 absorption/desorption measurement (Shimazu, ASAP2010).

The electrochemical measurement was carried out using the following procedure. The microelectrode used was a Pt-Rh filament (25 μm diameter) coated with Teflon. The microelectrode contacted a single particle dispersed on a glass frit in an electrolyte under microscope observations using a micromanipulator. As a control experiment, the composite electrodes were prepared by pressing a 12 mg mixture (the respective sample, acetylene black, and PTFE with 80:15:5 wt%) on a Ni mesh (9×6 mm^2). Li foil attached to a Ni mesh (9×6 mm^2) was used as a counter electrode and reference electrode. The electrolyte was 1 M $LiClO_4$ in a mixture of 50/50 vol% ethylene carbonate (EC) and propylene carbonate (PC) (Li ion battery grade, Mitsubishi Kagaku). All electrochemical measurements, i.e., cyclic voltammetry (CV) and the potential step methods, were carried out in a glove bag filled with air dried by a dryer (Balston, model 75-20).

Results and discussion

The XRD patterns of $LiCoO_2$ and the Mn-substituted samples are shown in Fig. 1. The simple phase assigned to the *R*-3*m* space group was observed for all of samples. No decrease in the ratio of the (003)/(104) diffraction peak intensities was obtained, which indicates no disordering of the Li, Mn, and Co cations in the layered structure with Mn content in the samples. However, the peak involving the information of the *c*-axis, e.g. the (003) peak, slightly shifted to a lower angle with an increase in Mn content. The calculated lattice constants of $LiCoO_2$ and $LiCo_{0.8}Mn_{0.2}O_2$ are shown in Table 1. While no difference in the length of the *a*-axis between the samples was observed, the length of the *c*-axis of $LiCo_{0.8}Mn_{0.2}O_2$ was slightly longer than that of $LiCoO_2$. This is attributed to the ion radius of Mn being bigger than that of Co^{3+}, and is consistent with the result of Stoyanova et al. [4]. It is noteworthy that the diffraction peaks become weaker and broader with the increase in Mn content, indicating a decrease in the crystal size.

The specific surface areas of the samples are also shown in Table 1. The specific surface area of $LiCo_{0.8}Mn_{0.2}O_2$ is clearly greater that of $LiCoO_2$, resulting from the decrease in the crystal size as mentioned above.

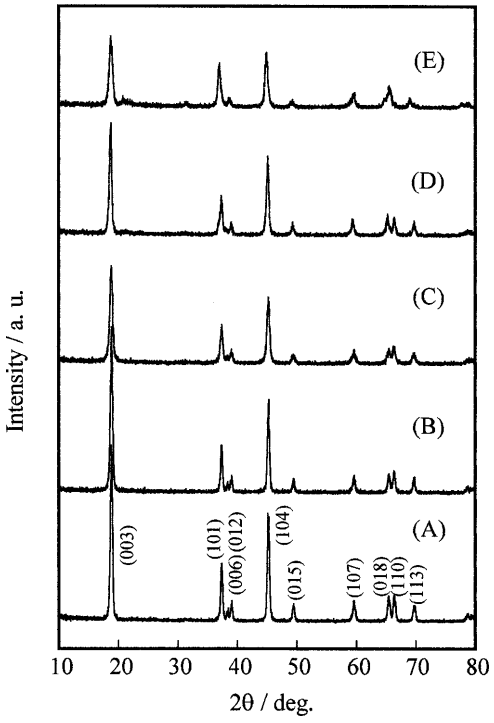

Fig. 1 Powder X-ray diffraction (XRD) patterns of the samples synthesized by the citrate process: **A** $LiCoO_2$, **B** $LiCo_{0.99}Mn_{0.01}O_2$, **C** $LiCo_{0.95}Mn_{0.05}O_2$, **D** $LiCo_{0.8}Mn_{0.2}O_2$, and **E** $LiCo_{0.5}Mn_{0.5}O_2$

Table 1 Calculated lattice constants and specific surface areas of $LiCoO_2$ and $LiCo_{0.8}Mn_{0.2}O_2$

Sample	Lattice constants		BET specific surface area (m^2/g)
	a (Å)	*c* (Å)	
$LiCoO_2$	2.816	14.05	7.4
$LiCo_{0.8}Mn_{0.2}O_2$	2.813	14.12	17.2

It should be noted that the specific surface area of $LiCoO_2$ synthesized by the citrate process was much greater than that made by the solid phase method [5]. It is known that the citrate process produces material having a small crystal size and a relatively high surface area [16].

Figure 2A shows a typical high-speed CV for a single particle of $LiCo_{0.8}Mn_{0.2}O_2$ (25 μm diameter), which was cycled between 3.0 and 4.3 V vs. Li/Li^+ at a scan rate of 10 mV/s for the 8th potential cycle. One set of peaks was mainly observed at ca. 3.9 V vs. Li/Li^+ in the CV. The separation between the anodic and cathodic peak was ca. 50 mV, indicating good reversibility. The CV shape for $LiCo_{0.8}Mn_{0.2}O_2$ is somewhat different from that for $LiCoO_2$, which shows three sets of peaks corresponding to Li^+ insertion/extraction with phase transitions of $LiCoO_2$ [9, 17]. This suggests that $LiCo_{0.8}Mn_{0.2}O_2$ is a single phase-transition material throughout the charge/discharge cycles in contrast to $LiCoO_2$. For the other Mn-substituted materials, although similar CVs were observed for a Mn content even at 1%, the broadness of

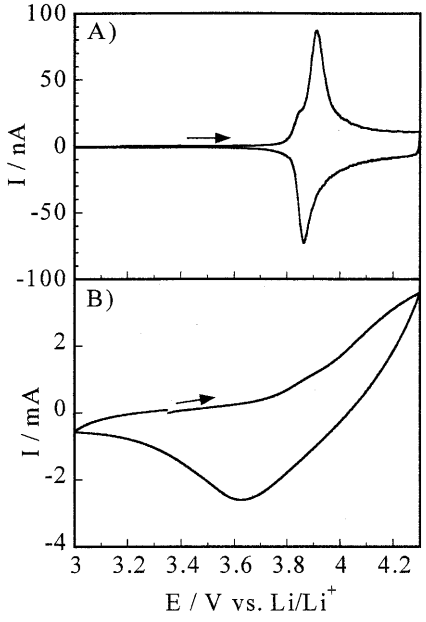

Fig. 2 Cyclic voltammograms for **A** a single particle of $LiCo_{0.8}Mn_{0.2}O_2$ (25 μm diameter) at 10 mV/s, and **B** a composite electrode consisting of $LiCo_{0.8}Mn_{0.2}O_2$, acetylene black, and PTFE with 80:15:5 wt% (total weight of the composite: 12 mg) at 1 mV/s in 1 M $LiClO_4$/PC + EC (1:1)

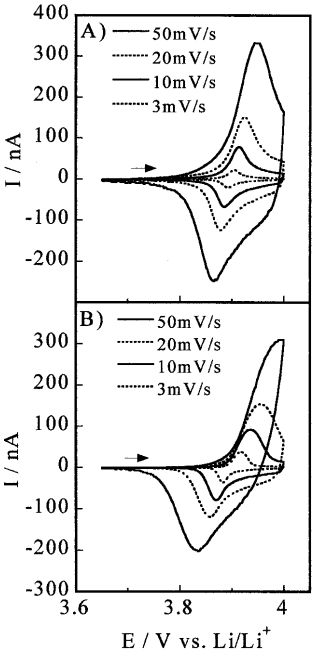

Fig. 3 Cyclic voltammograms for a single particle of **A** $LiCo_{0.8}Mn_{0.2}O_2$ (30 μm diameter) and **B** $LiCoO_2$ (21 μm diameter) at several scan rates (described in the figures) in 1 M $LiClO_4$/PC + EC (1:1)

the peak at 3.9 V was pronounced with an increase in the Mn content. Iltchev et al. [5] reported that the shape of the CV for $LiCo_{1-x}Mn_xO_2$ is similar to that for $LiCoO_2$ in the range of Mn substitution up to 4%, which is not in agreement with our results. Figure 2B shows the CV for the composite electrode of $LiCo_{0.8}Mn_{0.2}O_2$ as a control experiment. A peak-shaped CV was no longer observed at the scan speed of 1 mV/s because of the *iR* drop. Currents observed in the CV using the composite electrode are in the mA range, which are two orders of magnitude larger than those using the microelectrode. This is the reason why the distortion of the peak due to the *iR* drop was drastically improved using the microelectrode technique. To obtain the peak-shaped CV using the composite electrode, one has to measure it at a scan rate of 10 μV/s or less; however, the distortion of the anode and cathode peak in the CV is still much larger than that obtained by the microelectrode technique.

Figure 3A and B shows CVs obtained at different scan rates for the single particle of $LiCo_{0.8}Mn_{0.2}O_4$ (30 μm diameter) and $LiCoO_2$ (21 μm diameter), respectively. We have already reported that the kinetic reversibility and the cycle stability for $LiCoO_2$ depend on the reverse potential [9]. Accordingly, for both samples, the CVs were measured in the potential range between 3.6 and 4.0 V. The peak-shaped CV for $LiCo_{0.8}Mn_{0.2}O_2$ was obtained at a scan rate higher than 100 mV/s, while no clear peak for $LiCoO_2$ appeared even at 50 mV/s. The peak-shaped CV indicates that the scan rate used was sufficient to complete the oxidation/reduction of the entire material, which included the kinetic information for the insertion/extraction of Li^+ in the material. Consequently, Li^+ insertion/extraction in $LiCo_{0.8}Mn_{0.2}O_2$ seems to be faster than that in $LiCoO_2$. For $LiCo_{0.8}Mn_{0.2}O_2$, the peak current at ca 3.9 V was a linear relationship with the scan rate in the range less than 20 mV/s, but at the higher scan rates it deviated from the linear relationship, being close to a square root relationship. This suggests that the diffusion of Li^+ in the material can be controlled by the finite diffusion at the lower scan rates and by the semi-infinite diffusion at the higher scan rates. Similar behavior was obtained for $LiCoO_2$ in this study and in a previous study [9].

Based on a kinetic point of view, the potential step method was applied to single particles of $LiCoO_2$ and $LiCo_{0.8}Mn_{0.2}O_2$ to determine the apparent chemical diffusion constant (D_{app}) of Li^+ in the particles. D_{app} can be estimated from the following equation considering the spherical diffusion model, in which Li^+ diffuses from the surface to the center of a sphere [14, 18]:

$$\ln I = \ln(2FAC^*D_{app}/r) - (\pi_2 D_{app}/r^2)t \quad (1)$$

where A is the apparent surface area of the particles, C^* is the initial concentration of Li^+ in the particles, and r is the radius of the particles assuming a spherical shape. In this experiment, the electrode potential was stepped from 3.35 to 3.9 V for the Li^+ insertion. Figure 4A shows the anodic current response for $LiCoO_2$ (21 μm diameter). A clear current response was observed. When ln I vs. time was replotted from the obtained current response, a straight line was observed between 2 and 12 s as shown in Fig. 4B. From the slope of the line, D_{app} was calculated to be 2.6×10^{-8} cm^2/s, which is

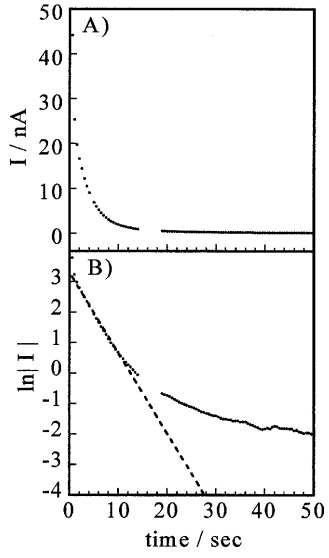

Fig. 4 **A** The anodic current response for $LiCoO_2$ (21 μm diameter) in 1 M $LiClO_4$/PC + EC (1:1) as the potential was stepped from 3.35 to 3.9 V vs. Li/Li^+. **B** Plot of ln *I* vs. *t* replotted from the obtained current response

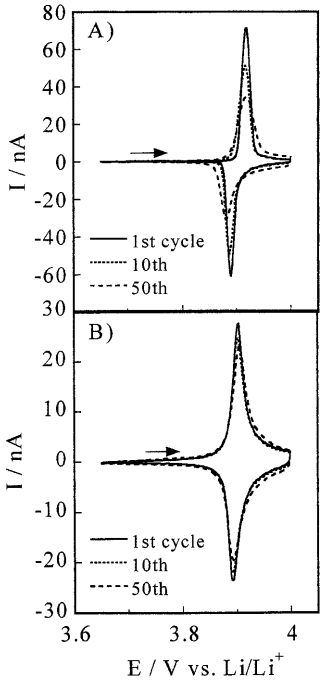

Fig. 5 Cyclic voltammograms for a single particle of **A** $LiCoO_2$ (21 μm diameter) and **B** $LiCo_{0.8}Mn_{0.2}O_2$ (30 μm) obtained by continuous potential cycles at 3 mV/s in 1 M $LiClO_4$/PC + EC (50:50 vol%). CVs obtained for 1st, 10th, and 50th cycles were only overlapped in the figures

consistent with some reported values [19–21] but inconsistent with others [22, 23]. In contrast, the D_{app} of $LiCo_{0.8}Mn_{0.2}O_2$ calculated in the same manner was 6.4×10^{-8} cm^2/s. The difference in D_{app} indicates that the process of Li^+ insertion/extraction in $LiCo_{0.8}Mn_{0.2}O_2$ is more convenient than that in $LiCoO_2$, which is probably due to the expansion of the *c*-axis and/or the decrease in the crystal size for $LiCo_{0.8}Mn_{0.2}O_2$, as shown in Table 1. It should be noted that the calculated D_{app} increased with an increase in Mn content up to $x = 0.2$, and then decreased at $x = 0.5$.

To clarify the stability of the material during cycling, CVs of the single particle of $LiCoO_2$ (21 μm diameter) and $LiCo_{0.8}Mn_{0.2}O_2$ (30 μm diameter) were obtained from continuous scanning at 3 mV/s in the potential range between 3.65 and 4.0 V, as shown in Fig. 5. In the case of $LiCoO_2$ (Fig. 5A), a marked decrease in the peak current (71 to 34 nA) and an increase in the half-peak width (19 to 34 mV) were observed with potential cycles. However, the amount of charge passed between 3.65 and 4.0 V was independent of the potential cycles, indicating that the peak became only broader. In addition, the peak potential slightly shifted toward the higher potential with an increase in the number of cycles. These results indicate some kinetic deterioration of the Li^+ insertion/extraction in $LiCoO_2$. Ohzuku et al. [24] have reported that the *c*-axis length of $LiCoO_2$ changed from 14.08 to 14.26 Å on either side of the intense peak at ca. 3.9 V vs. Li/Li^+. The repetition of changing the *c*-axis length might lead to the fatigue of the structure of $LiCoO_2$, which is most likely the explanation for the above results. On the other hand, for $LiCo_{0.8}Mn_{0.2}O_2$ (Fig. 5B), not only a decrease in the peak current and an increase in the half-peak width but also a shift in the peak potential was only slightly observed. This indicates the excellent cycle stability of $LiCo_{0.8}Mn_{0.2}O_2$, namely, an improvement in the cycle stability of $LiCoO_2$ by substituting part of Co with Mn. The increase of the *c*-axis length by Mn substitution shown in Table 1 may moderate the structure change of $LiCoO_2$ with the repetition of Li^+ insertion/extraction, while further studies are necessary for a complete understanding of the behavior. Note that the cycle stability was worse as the Mn content deviated from 20%, showing that $LiCo_{0.8}Mn_{0.2}O_2$ should be the most suitable candidate for cathode materials among the Mn-substituted compounds in this study.

Conclusion

The objective of the present study was to realize the electrochemical properties of $LiCo_{1-x}Mn_xO_2$ alone, synthesized by the citrate process, using the microelectrode technique. From an electrochemical point of view, the CVs for the Mn-substituted materials gave one set of peaks at 3.9 V vs. Li/Li^+ and were different from that for $LiCoO_2$. Furthermore, the CVs made it clear that the increase in the Mn substitution up to 20% lead to an improvement in the cycle stability of the $LiCoO_2$. The potential step experiment revealed a difference in the D_{app} of Li^+ between $LiCo_{0.8}Mn_{0.2}O_2$ (6.4×10^{-8} cm^2/s) and $LiCoO_2$ (2.6×10^{-8} cm^2/s).

Based on these considerations, it is recommended to select $LiCo_{0.8}Mn_{0.2}O_2$ as one of the promising cathode materials for a 4 V class secondary lithium battery. We believe that it is extremely important to realize the electrochemical properties of only the battery active materials for designing a high-performance secondary battery.

References

1. Nagaura T, Tazawa K (1991) Prog Batt Solar Cells 9: 209
2. Mizushima K, Jones PC, Wiseman PC, Goodenough JB (1980) Mater Res Bull 15: 783
3. Tukamoto H, West AR (1997) J Electrochem Soc 144: 3164
4. Stoyanova R, Zhecheva E, Zarkova L (1994) Solid State Ionics 73: 233
5. Iltchev N, Bowden W, Moses PR (1997) Electrochem Soc Proc 96-17: 235
6. Jones CDW, Rossen E, Dahn JR (1994) Solid State Ionics 68: 65
7. Ohzuku T, Ueda A, Nagayama M, Iwakoshi Y, Komori H (1993) Elctrochim Acta 38: 1159
8. Ueda A, Ohzuku T (1994) J Electrochem Soc 141: 2010
9. Uchida I, Fujiyoshi H, Waki S (1997) J Power Sources 68: 139
10. Nishizawa M, Uchida I (1999) Electrochemistry 67: 420
11. Dokko K, Nishizawa M, Uchida I (1998) Denki Kagaku 66: 1188
12. Nishizawa M, Hashitani R, Itoh T, Matsue T, Uchida I (1998) Electrochem Solid State Lett 1: 10
13. Ura H, Nishina T, Uchida I (1995) J Electroanal Chem 396: 169
14. Nishina T, Ura H, Uchida I (1997) J Electrochem Soc 144: 1273
15. Nishizawa M, Koshika H, Uchida I (1999) J Phys Chem B 103: 192
16. Baythoun MSG, Sale FR (1982) J Mater Sci 17: 2757
17. Reimers JN, Dahn JR (1992) J Electrochem Soc 139: 2091
18. Bard AJ, Faulkner LR (1986) Electrochemical methods, chap. 5. Wiley, New York
19. Thomas MGSR, Bruce PG, Goodenough JB (1985) Solid State Ionics 17: 13
20. Pyun S-I, Choi Y-M (1997) J Power Sources 68: 524
21. Choi Y-M, Pyun S-I (1998) Solid State Ionics 109: 159
22. Mizushima K, Jones PC, Wiseman PJ, Goodenough JB (1981) Solid State Ionics 3/4: 171
23. Aurbach D, Levi MD, Levi E, Teller H, Markovsky B, Salitra G, Heider U, Heider L (1998) J Electrochem Soc 145: 3024
24. Ohzuku T, Ueda A (1994) J Electrochem Soc 141: 2972